

¹ DRAFT VERSION FEBRUARY 4, 2019

Corresponding author: Felipe Leonardo Gómez-Cortés
fl.gomez10@uniandes.edu.co

Typeset using L^AT_EX **preprint** style in AASTeX62

Weekly Activity Report

Week 1

A first algorith comparing two β -Skeletons

FELIPE LEONARDO GÓMEZ-CORTÉS¹

MASTER STUDENT

—

JAIME E. FORERO-ROMERO¹

ADVISOR

¹*Physics Department, Universidad de Los Andes*

ABSTRACT

The beta parameter graph and its definition.

The testing catalogs.

How the graph changes while varying β .

How this first attempt fails over very excentric ellipsoidal voids.

Keywords: Beta Skeleton Graph, Beta Parameter

1. THE ALGORITHM

The algorith uses the NGL library to create two β -Skeleton graph of a given set of points, and comparing the differences between them to identify the voids in the structure of points.

The graphs of the 0.9-Skeleton and the 1-Skeleton are calculated, then compared. Each lenght is measured and the histogram of connection lenghts is created for both β values. (in a similar fashion to the two-point correlation function) By removing the short connections -common in both skeletons-, and preserving the long connections -those that cross through the voids-, the points envolving the voids are identified.

1.1. *Mock Catalog*

In order to test the algorith, three catalogs of points in a 3D space where created with empty regions emulating voids in the LSS.

The emulated space is a cubic region of 60 Mpc/h. There where placed $\sim 5 \times 10^4$ points to have a similar volume density of points to the halo volumetric density in the AbacusCosmos simulations. (8.7×10^6 halos in a cubic box of 720 Mpc/h length, 2.335×10^{-2} halo/(Mpc/h)³). Points where placed using an uniform density probability distribution.

Then, using the equation for the sphere and the ellipsoid, the subset of points within the surface is removed from the catalog.

The first set of points has an spherical empty region of radius 20 Mpc/h centered in the middle of the volume.

The second catalog has four non-overlapping spherical empty regions of radius between 8 and 20 Mpc/h.

The third catalog has four overlapping ellipsoidal voids.

1.2. The β -Skeleton Graph

The β -Skeleton graph is defined by the relative distance between points (vertices) in a N-dimensional space, and a geometrical criterion using a real parameter $\beta \geq 0$. This graph is not directed, there is no a preferential direction in the edges connecting vertices.

The geometrical criterion is the following: two points (p, q) are connected in the graph if there is an empty region between them, without any other point. The shape of the empty region is function of the β /parameter and the distance $d(p, q)$ between the points. In the case $\beta = 0$ the empty region is a N-ball of diameter d centered in the midpoint between

The NGraph authors define the β -skeleton as follows:

“The so-called lune-based β -skeleton is a one-parameter generalization of the RNG [Relative Neighborhood Graph] and GG [Gabriel Graph], defined as follows:

- For $0 < \beta < 1$, the empty region is the intersection of all d-balls with diameter $d(p, q)/\beta$ that have p and q on the boundary.
- For $\beta \geq 1$, the empty region is the intersection of two d-balls with diameter $\beta d(p, q)$ centered at $(1 - \frac{\beta}{2})p + \frac{\beta}{2}q$ and $\frac{\beta}{2}p + (1 - \frac{\beta}{2})q$.”

In the limit when β tends to zero, every point is connected to each point on the set, it corresponds to the graph used in the classic two-point correlation function. Each point has N connections. (With N as the number of points in the set).

When β is increasing, the number of connections per point is reduced. The first connections to vanish are the longer ones, while the short connections persists.

2. STRUCTURE DEPENDENCE OF β PARAMETER

By the nature of its definition, the β -skeleton structure changes with the continuous β parameter, from a highly connected structure (when $\beta \rightarrow 0$) to an empty graph when β grows to large positive values.

The Skeleton, the number of connections per point, and the length of connections, they depend also from the distribution of points in the space. Is expected to have different values for the cosmic web, but is necessary to have a testing catalog with well known structures to test the algorithm.

The testing set was generated using a uniform density probability to place the points inside the box. There is a transition in the Skeleton of this catalog when β is close to 1, it is shown in the figure 1. Small β values allows the large connections in the skeleton. (a, b and c). When $\beta \geq 1$ the large connections through the spherically uniform void vanish.

3. DETECTING THE FIRST VOID

The 0.9 and 0.99-Skeleton were calculated and compared with the 1-Skeleton. The histograms of number of connections per point (figure 2) show that the 1-Skeleton the nodes tend to have 7 connections, while for the 0.9 and 0.99-Skeletons the mean goes around 16 and 10 connections per node respectively. This graph may be useful in advanced stages of this project, it doesn't give more information than the Skeletons were successfully constructed by the NGRAPH library.

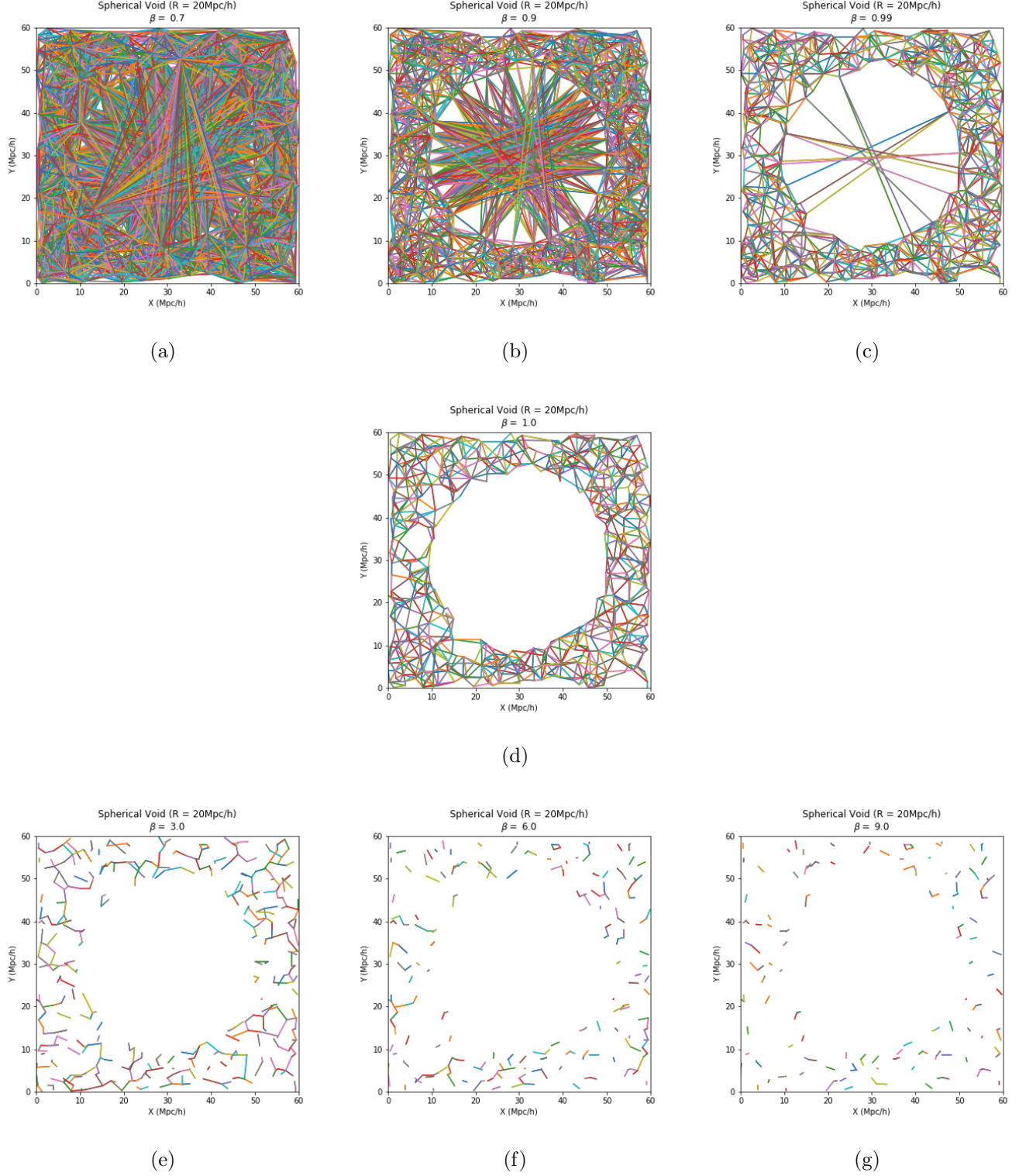


Figure 1. Skeleton Structure dependence of β around a single void. Seven different values for β (0.7, 0.9, 0.99, 1, 3, 6, and 9). A transition can be observed when $\beta \rightarrow 1^-$.

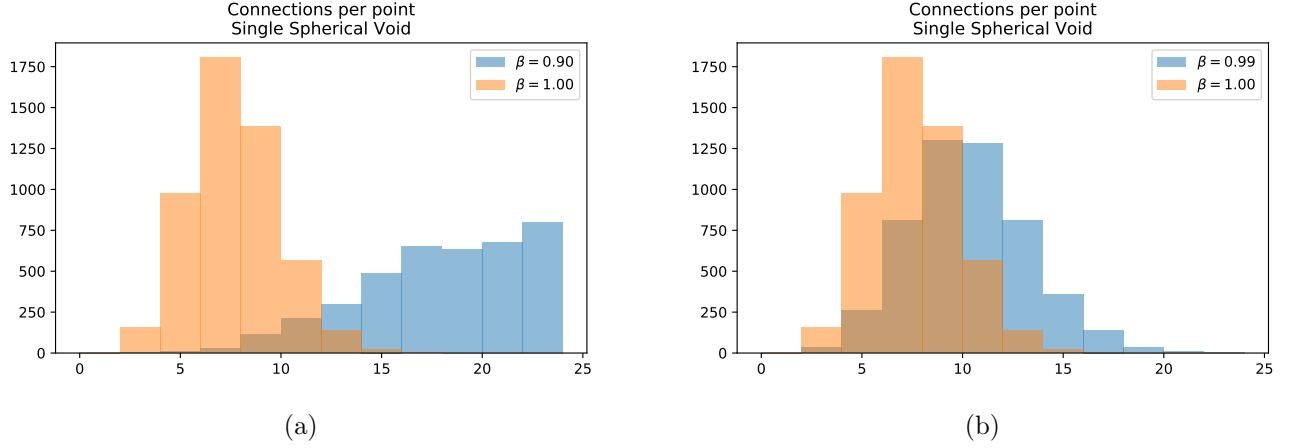


Figure 2. Connections per point.

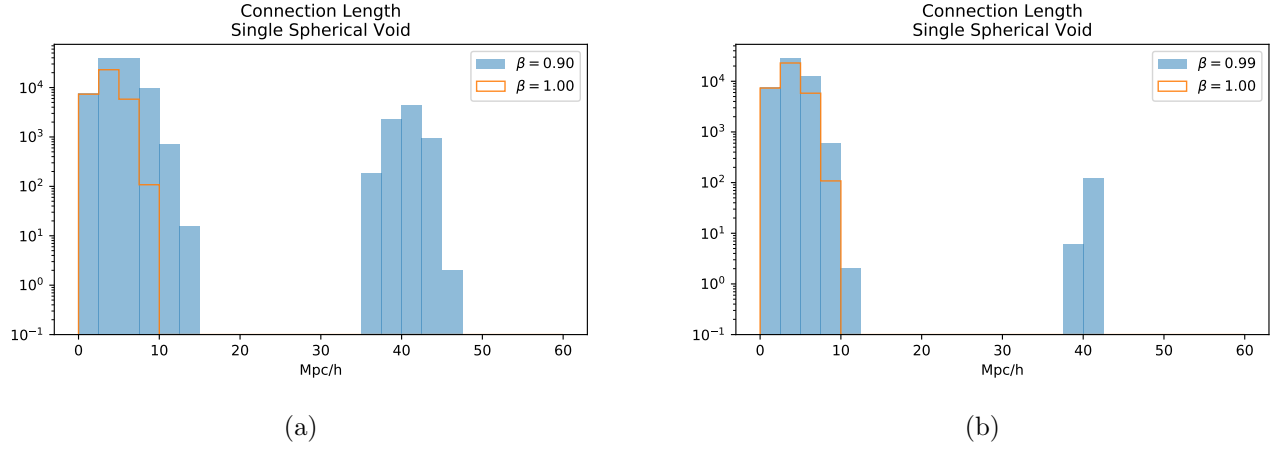


Figure 3. Length connection for different β values.

More information can be inferred by analyzing the histograms of connection lengths (figure 3): the 1-Skeleton has short connections, none of them larger than the radius of the spherical void ($R=20\text{Mpc/h}$). But 0.9 and 0.99 Skeletons show a peak close to the diameter of the void in the testing catalog.

3.1. Selecting Surface Points

Once the typical length for the 1-Skeleton is detected, a low limit distance can be established to separate long and short distances. **This d_{cut} was hand-selected** as $d_{cut} = 20\text{Mpc/h}$. The histograms a and b in figure 3 show a second point close to the diameter of the void. By keeping the nodes with connections around that value (40 Mpc/h), and discarding the short connections, the surface enclosing the void appears (figure 4). This method is good enough for a single spherical void in a random set of points.

3.2. Detecting Multiple Spherical Voids

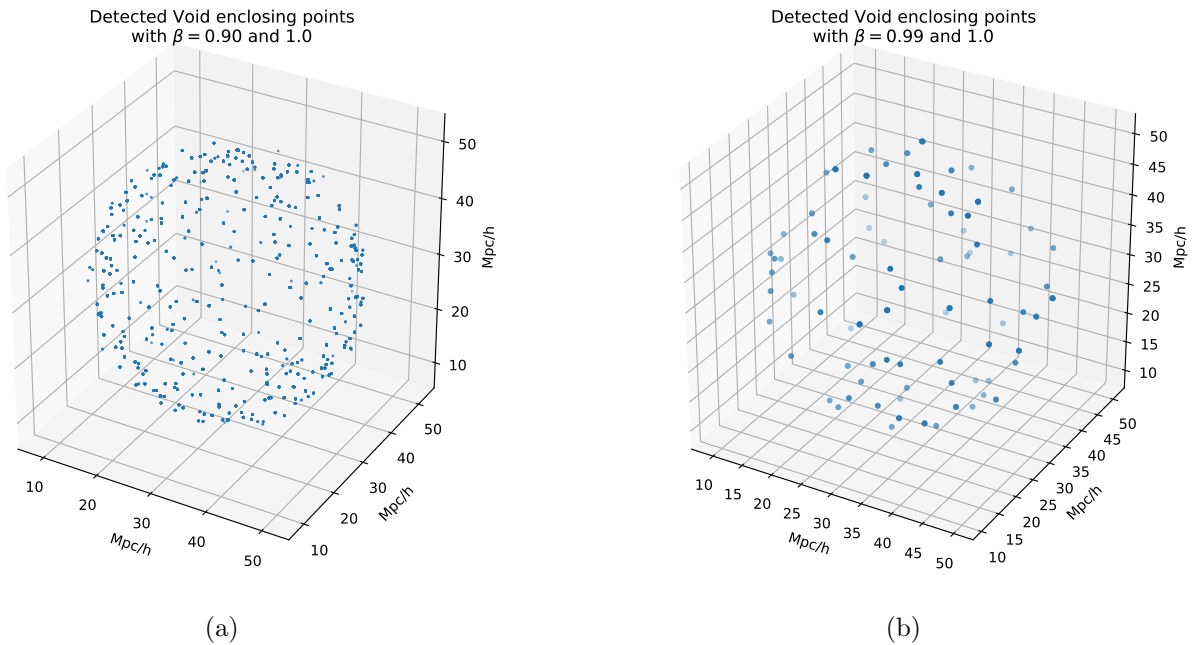


Figure 4. Surface points enclosing the void choosen by comparing connection lenghts in the 0.90 and 0.99-Skeleton versus the 1-Skeleton.

The testing catalog used has four non-overlapping spherical voids with different radius (10, 10, 12 and 20 Mpc/h) in the same cubic box of 60 Mpc/h length.

The connection lenght histograms show the short connections for regular populated space (all the contribution for the 1-Skeleton) and the large connections for $\beta < 1$, with peaks around the diameter of the voids, as expected. (Figure 5)

The difference between the voids and the populated structure is visible at $\beta = 0.99$; three different clusters appears in the rigth panel. But in the left panel, the two bells are overlapping. There is no a clear difference between the low scale connections and connections through voids. (May it be visible with another bin selection?)

Again, the limit between short and large connections is handmade selected as $d_{cut} = 15\text{Mpc/h}$.

With this handmade selection of long connections, the algorithym sucesfully identifies the four voids (figure 8).

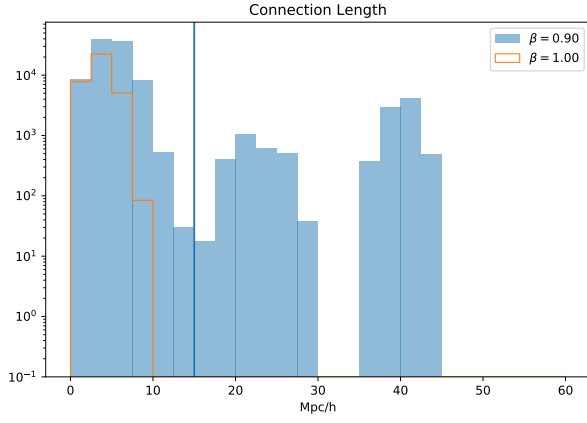
4. THE ELLIPSOIDAL CATASTROPHE

Trying to give a leap, instead going step by step, the third catalog of points includes three connected ellipsoidal voids, varying the coefficients in the standard ellipsoid equation between 0.5 and 2.0. The algorithym fails to identify the ellipsoidal voids, but detects the spherical control void.

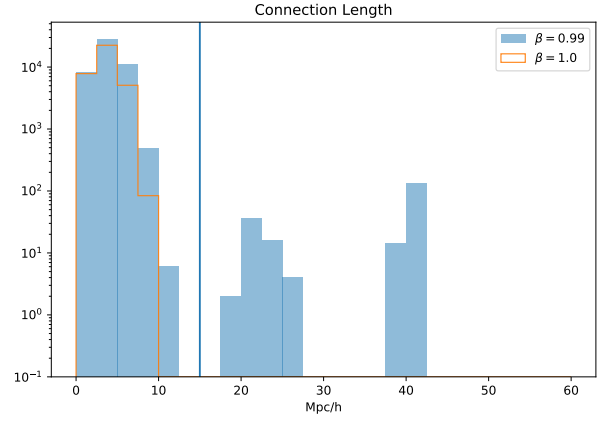
5. CONCLUSIONS

An important factor as d_{cut} cannot be arbitrarily selected.

REFERENCES

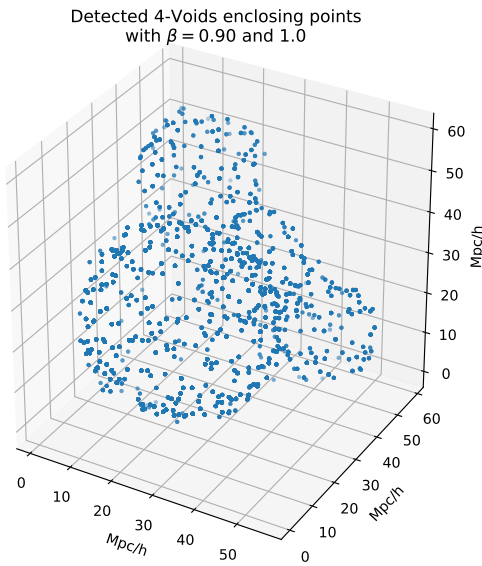


(a)

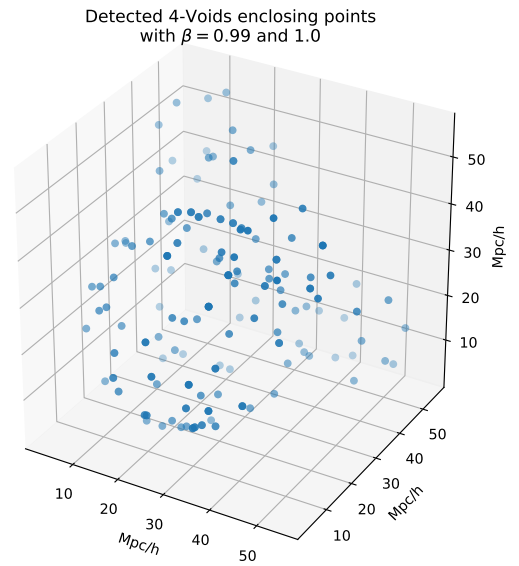


(b)

Figure 5. Length connection for different β values with four voids inside the structure. Diameter of the voids: 20, 20, 24 and 40 Mpc/h.

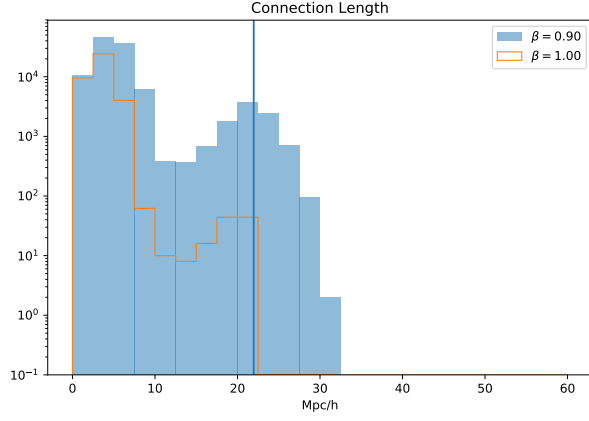


(a)

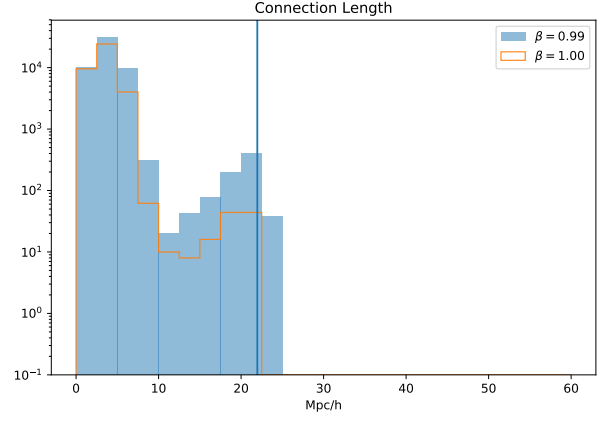


(b)

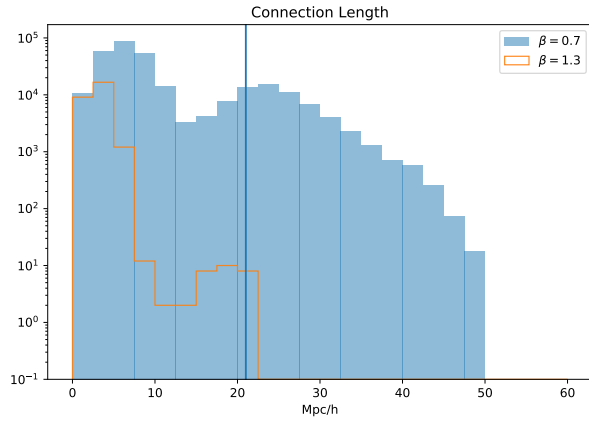
Figure 6. Surface points enclosing the four void chosen by comparing connection lengths in the 0.90 and 0.99-Skeleton versus the 1-Skeleton.



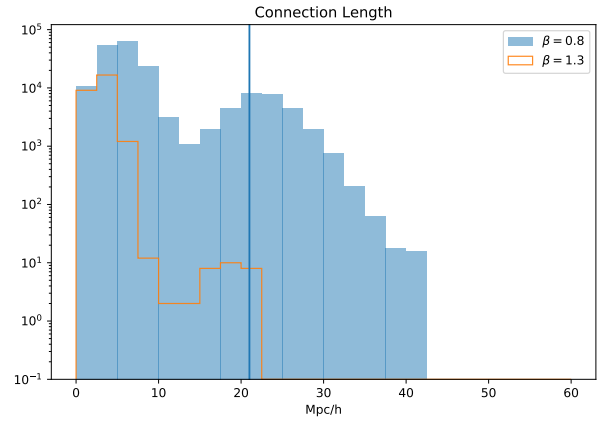
(a)



(a)



(c)



(d)

Figure 7. Length connection for different β values with four connected ellipsoidal voids. There is no a clear difference in the histograms about connection length in populated space and empty regions. Upper Panels: using the previous β difference comparing against 1-Skeleton, it worked for spheroidal voids, but not for connected ellipsoidal voids. Lower panels: increasing the β difference, comparing against 1.3-Skeleton.

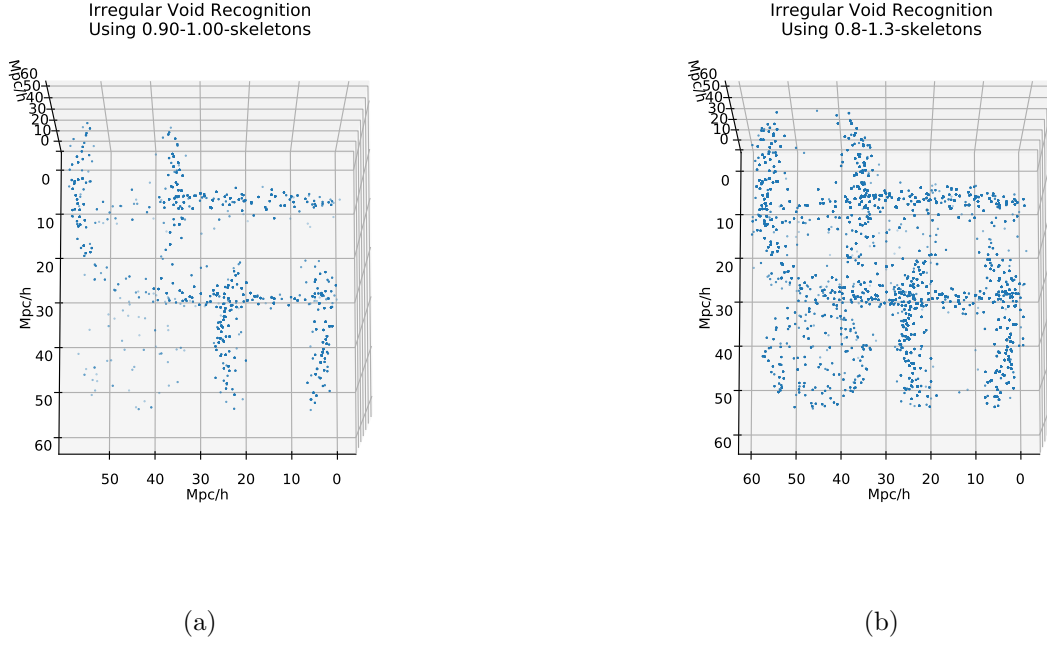


Figure 8. Surface points enclosing the four connected ellipsoidal voids chosen by comparing connection lengths in the 0.90-Skeleton versus the 1-Skeleton (left panel). There is a notable lack of points in the upper and lower regions of the ellipsoids, as the front and the bottom. The algorithm fails to identify the spheroidal voids in the structure. In the right panel there is an intent to fix the issue using a larger difference in the β values, using the 0.8 and 1.3-Skeletons. The algorithm stills without identify the voids.